

# 

# PROGRESS REPORT: VENT PROCESSES DURING THE 1912 ERUPTION AT NOVARUPTA, KATMAI NATIONAL PARK, ALASKA

June 1, 1993

Terri Bates, John Eichelberger, and Sam Swanson

#### Abstract

Blocks of welded fragmental material ejected at Novarupta during the great eruption of 1912 provide evidence of the contents and development of the vent. Because they appear to represent material held at magmatic temperature for hours to days and then quenched at depth and ejected, they provide unusual information on the timing of processes of degassing, welding, and magma mixing. Two breccia types are distinguished by proportions of the three magmatic components. Type 1 breccia (Hildreth's "vitrophyre") is rhyolite- and andesite-rich ("volcanic inclusions" in the glassy matrix were found to be 1912 andesite), contains abundant lithics, and is found throughout deposits of the eruption's second and third days. It corresponds to magmatic proportions being erupted toward the end of the first day, or Episode I. Type 2 is dacite-rich and poor in lithics, and occurs only at the surface. It corresponds to magmatic proportions erupted during Episodes II and III. A pyroclastic dike exposed in a bomb of Type 2 vent breccia is petrologically related to Novarupta lava. Water is strongly but not completely degassed from vent breccias (Type 1 breccia at 0.30 wt. % H<sub>2</sub>O and Type 2 breccia at 0.15 wt. % H<sub>2</sub>O even when bread crusted) and more thoroughly degassed from dome lava (rhyolite and andesite at <0.10 wt. % H<sub>2</sub>O), but the pyroclastic dike retains significant water (averages 0.90 wt. % H<sub>2</sub>O) and its host breccia likewise contains elevated water concentrations (0.30-0.40 wt. % H<sub>2</sub>O). The mafic component in Novarupta dome is derived from andesitic, rather than dacitic magma, and has crystallized substantially in response to mixing with its cooler host.

We infer that above the fragmentation level (calculated to be about 500 m depth following assumptions of Sparks, 1978), the vent should consist of an annulus of Type 1 material, formed during backfilling of the vent during the close of Episode I, enclosing an inner cone of Type 2 material formed similarly during waning stages of Episodes II/III. Although occurrence of Falling Mountain material in Type 1 requires some downward motion of components comprising the breccia, the modestly elevated water contents, fines-depleted nature, and textural contrasts to ignimbrite suggest that Type 1 may not be simply fall-back, but could represent material aggraded on vent walls at depth, resulting in gradual constriction of the vent. If so, the dike-bearing breccia is the deepest-derived sample. Ejection of such material without vesiculation suggests quenching in situ, which in turn suggests invasion of ground water into the vent during the eruption. The pyroclastic dike provides evidence that intrusion of Novarupta lava began immediately after the explosive phase (otherwise, the host breccia would be devitrified; devitrification of Novarupta began before extrusion ceased). It also suggests a possible mechanism for formation of thin dikes of viscous magma at shallow depth: hydrofracturing with injection of magmatic dusty gas. Drilling will likely begin in devitrified equivalents of Type 2 breccia and the slant hole should encounter the devitrified equivalent of Type 1, and perhaps quenched, glassy Type 1, before reaching the vent wall.

#### DISCLAIMER

This report was prepared as an account of work sponsored by an agency of the United States Government. Neither the United States Government nor any agency thereof, nor any of their employees, makes any warranty, express or implied, or assumes any legal liability or responsibility for the accuracy, completeness, or usefulness of any information, apparatus, product, or process disclosed, or represents that its use would not infringe privately owned rights. Reference herein to any specific commercial product, process, or service by trade name, trademark, manufacturer, or otherwise does not necessarily constitute or imply its endorsement, recommendation, or favoring by the United States Government or any agency thereof. The views and opinions of authors expressed herein do not necessarily state or reflect those of the United States Government or any agency thereof.

MASTER

dis

DISTABUTION OF THIS DOC IMENT IS UNLIMITED

# **Background**

The largest eruption of this century burst from Novarupta in the Aleutian Arc on June 1912. Several authors (Griggs 1922; Curtis, 1968; Hildreth 1983, 1987; Fierstein and Hildreth 1992) have contributed to current understanding of the eruption chronology and stratigraphy. The new vent erupted three distinct magmas and deposited nearly 30 km<sup>3</sup> of air-fall tephra and ignimbrite. The steaming ash flow sheet covered lowlands up to 23 km from the vent and earned the title of Valley of Ten Thousand Smokes from explorers years after the eruption.

The approximately 60 hours of volcanic activity began with a rhyolite-dominant pulse that contemporaneously emplaced a regionally extensive Plinian fallout unit and an ignimbrite sheet. During this first episode, dacite and andesite components gradually increased and dominance in eruptive style shifted from plinian column to pyroclastic flow. The predominantly dacitic eruptions of Episodes II and III deposited Plinian air fall units and minor ash flows and surges. Andesite-contaminated rhyolite lava of Novarupta Dome was emplaced following the end of the Plinian eruptions.

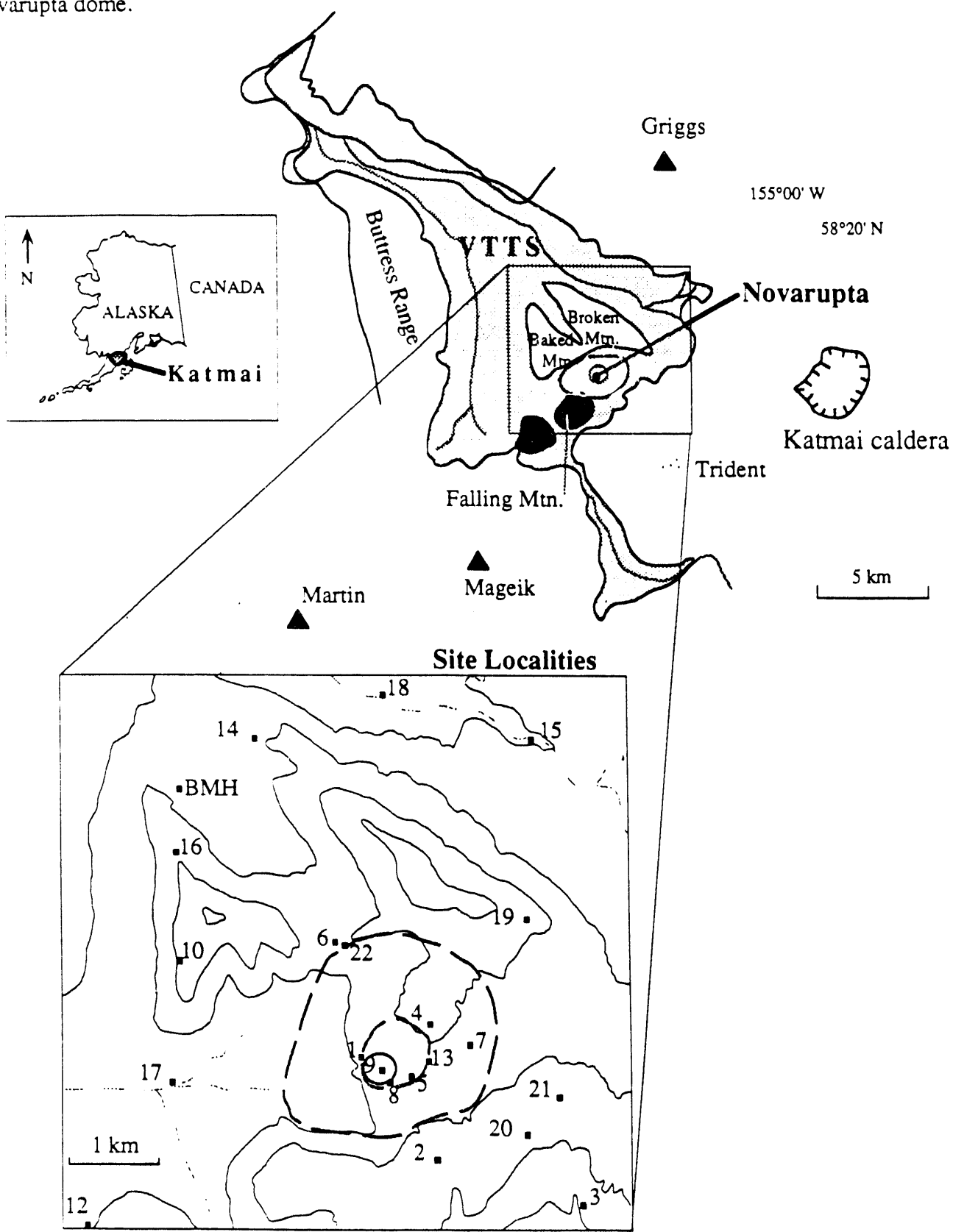
Episode I opened a new vent through bedrock of sedimentary Naknek Formation. Syneruptive reaming and slumping expanded the conduit to a flaring, funnel-shaped vent about 2 km wide at the surface (Hildreth 1983; Eichelberger et al. 1991; Goodliffe et al. 1991). A several hour break followed Episode I. Growth of the vent truncated ridges of Naknek Formation comprising parts of Baked and Broken Mountains, and a Holocene dacitic dome, Falling Mountain (Fig. 1). The 400-m-diameter vent of Episodes II and III is thought to be wholly nested within the Episode I crater. In turn, last-emplaced Novarupta Dome lies within the Episode II/III vent.

Hildreth (1987) noted lithics of dark vitrophyre in the 1912 post-ignimbrite deposits. Many clasts contain inclusions of oxidized volcanic and basement rocks within an unaltered glassy matrix. He suggested tephra fell back into the vent, welded and was subsequently reejected as this volcanic breccia. These are complex rocks because they contain, or potentially contain, the three magmatic components of the 1912 eruption as well as wallrock lithologies. They are important because of the baseline information they provide regarding the contents of the vent and because their P-T-t history is unusual and well constrained. Together with airfall tephra and lava, they comprise a suite of materials that underwent rapid decompression and rapid cooling (tephra), rapid decompression then held at temperature for 1-2 days then quenching (breccia), and slow decompression and cooling (lava). How these different paths affect degassing, crystallization, and mixing is now under investigation.

#### Approach

The first step in understanding the breccias was a field investigation of what kinds of breccias occur and how they are distributed within the deposits. The next step was an optical and electron microprobe investigation to identify their components. Analysis for retained volatiles was undertaken concurrently. Future work will use microbeam techniques to look in detail at the distribution of water in order to test degassing concepts, and image analysis to track the crystallization response of the magmas.

Figure 1. Novarupta Volcano is located in Katmai National Park on the Alaska Peninsula. The Valley of Ten Thousand Smokes (VTTS) is composed of ash flows associated with the 1912 eruption. Sample and measurement sites are displayed in the enlarged vent area map. Heavy dashed lines represent surface outlines of the Episode I (outer) and Episodes II-III (inner) vents. The heavy circle within the vent is Novarupta dome.



# Breccia components

Novarupta vent breccias consist of varied proportions of 1912 rhyolite, dacite and andesite clasts and may or may not contain lithic fragments of sedimentary Naknek Formation and Falling Mountain dacite. Two breccia types were defined based on field estimates of phenocryst and lithic content. Lithic-rich, crystal-poor clasts were designated Type 1 and crystal-rich, lithic-poor Type 2. Important sample and observation sites in the vent area are displayed in Figure 1. Weight percentage of each pumice and lithic type were measured for individual beds in several vertical sections; bulk samples were taken from an area the height of the unit by ~half meter wide and ~10 cm into the section (after scraping the weathered surface clean); all clasts >1 cm were sorted by type and weighed in bags with hand-held scales; [a few questionable clasts were returned to the lab where a fresh-cut surface allowed accurate identification]. Vertical sections contain only Type 1 breccia below the surface (Fig. 2).

Breccia clasts collected from the surface of several 4 m<sup>2</sup> grids were sorted by type and weighed in bags suspended from hand-held scales. Type 2 appeared to be the dominant breccia on the surface except where wind ablation exposed Type 1 from the underlying deposits (Fig. 3). Ablated areas have lost significant amounts of pumice easily swept away by strong winds in the area: note sites 6 and 22 in particular. The surface layer of Type 2 breccia is undisturbed at site 6, but within tens of meters at site 22, ablation has uncovered a significant amount of Type 1 breccia. Surface counts thus do not always represent purely surface deposition. Significantly, Type 1 first appears toward the end of Episode I deposits and Type 2 is restricted to the surface layer.

# Density

Bulk densities of large samples of Type 2 breccia and rhyolite dome lava were measured in the field. Samples of visibly different vesicularity were collected and weighed initially in air and then suspended in water. Density was calculated by the following expression:

$$\rho = [1-(\text{weight in water})/(\text{weight in air})]^{-1}.$$

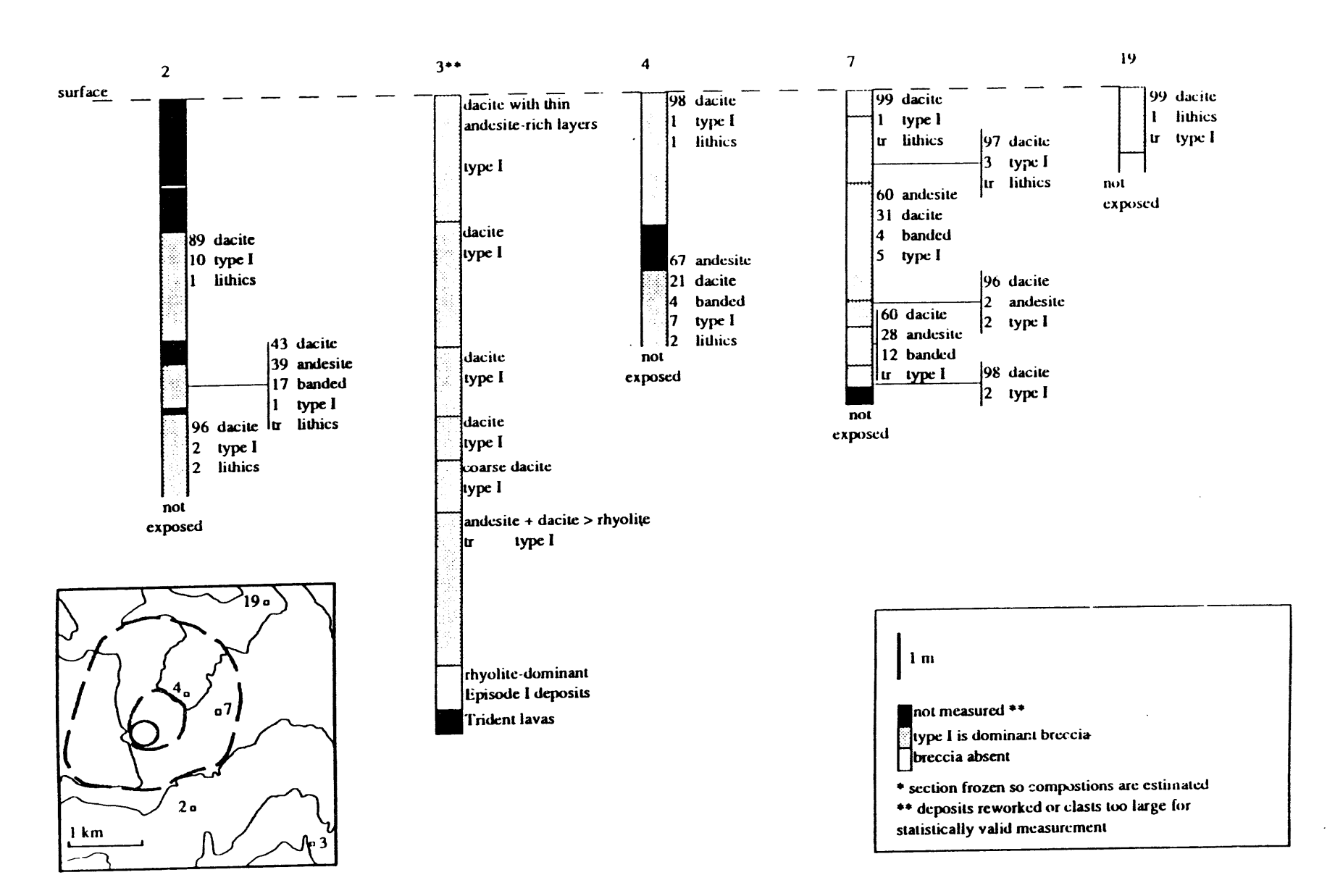
As it was not possible to dry samples before weighing, calculated bulk densities are an upper limit which will be close to true values at low porosity. Porosity was calculated using the bulk density of nearly vesicle-free samples as the grain density.

#### Petrography

Detailed investigation of samples collected from a number of sites (1 - 7) permitted a better understanding of characteristics of the two breccia types. Type 1 breccia occurs as up to 30 cm blocks of dark obsidian with relatively few phenocrysts, ~5-15%. Lithics comprise ~15% of Type 1 although some samples are essentially lithic-free; Naknek Formation and Falling Mountain dacite are by far the most common lithic types. Comparison to 1912 pumices in point counting and by component analysis of whole rock data establish Type 1 magmatic proportions as andesite (57%) > rhyolite (34%) >> dacite (9%). Some andesite clasts have significantly more crystalline groundmass than is typical for the andesite pumice. The large component of crystal-poor rhyolite explains the scarcity of phenocrysts in Type 1. Mean pumice clast size is approximately 3 mm; no interstitial dust is present and bubble wall shards are rare. Most pumice clasts exhibit a great amount of compaction. Rhyolite and dacite clasts average 8:1 elongation but andesite is considerably less compacted. Partially compacted, vesicular Type 1 fragments first appear in the late andesite-rich ignimbrite of Episode I (Fig. 2). Examination of sintered ignimbrite exposures in Knife Creek and River Lethe (sites 15, 17 and 18 in Fig. 1) revealed no

GI 91-91b

Figure 2. Stratigraphic sections of near vent deposits are numbered according to site location. Presence of lithic breccia fragments is emphasized.



measured area from the vent center (here taken to be the central pit in Novarupta dome). Numbers refer to site localities mapped in Figure 1. 14 **夕1612** sitesdistance from vent (km) **19** ♦ 21 20 22 ~ 9 13 5 20-8 8 9 wt. % breccia

Figure 3. Ratios of type I to type II breccia at the surface of 1912 deposits are displayed. Sites are arranged according to lateral distance of

breccia clasts. The typical densely welded Type 1 form is not found until Episode II deposits, where it comprises up to 10 wt. % of individual beds.

Type 2 breccia is variably welded, crystal-rich (~15-30% phenocrysts), lithic-poor and forms up to 2 m blocks. Naknek Formation and Falling Mountain dacite as well as Type 1 lithics occur in Type 2. A wide range of density represents variable welding in Type 2 samples (Fig. 4). Proportions of 1912 magmatic components are dacite (60%) > andesite (37%) >> rhyolite (3%) based on point counts and component analysis of whole rock data. Pumice clasts average ~10 mm; neither dust nor bubble wall shards are present. Type 2 exists only on the surface of the 1912 tephra section; Type 2 is concentrated in tephra ring and includes both large bread-crusted bombs and dense blocks, many of which appear on casual inspection to be lava-like rather than fragmental material.

# Tephra dike

One breccia block, assigned to Type 2 based upon high crystal content and low rhyolite content but richer in andesite than normal Type 2, contains a dike of light gray glass similar to 1912 rhyolite in color. When point-counted, rhyolite pumice contains 1.4% crystals, rhyolite lava 2.5% crystals, but dike material 21.5% crystals, the origin of which are discussed later. In thin section, this dike has a pyroclastic texture of glass with distinctive fiamme and many fragmented crystals.

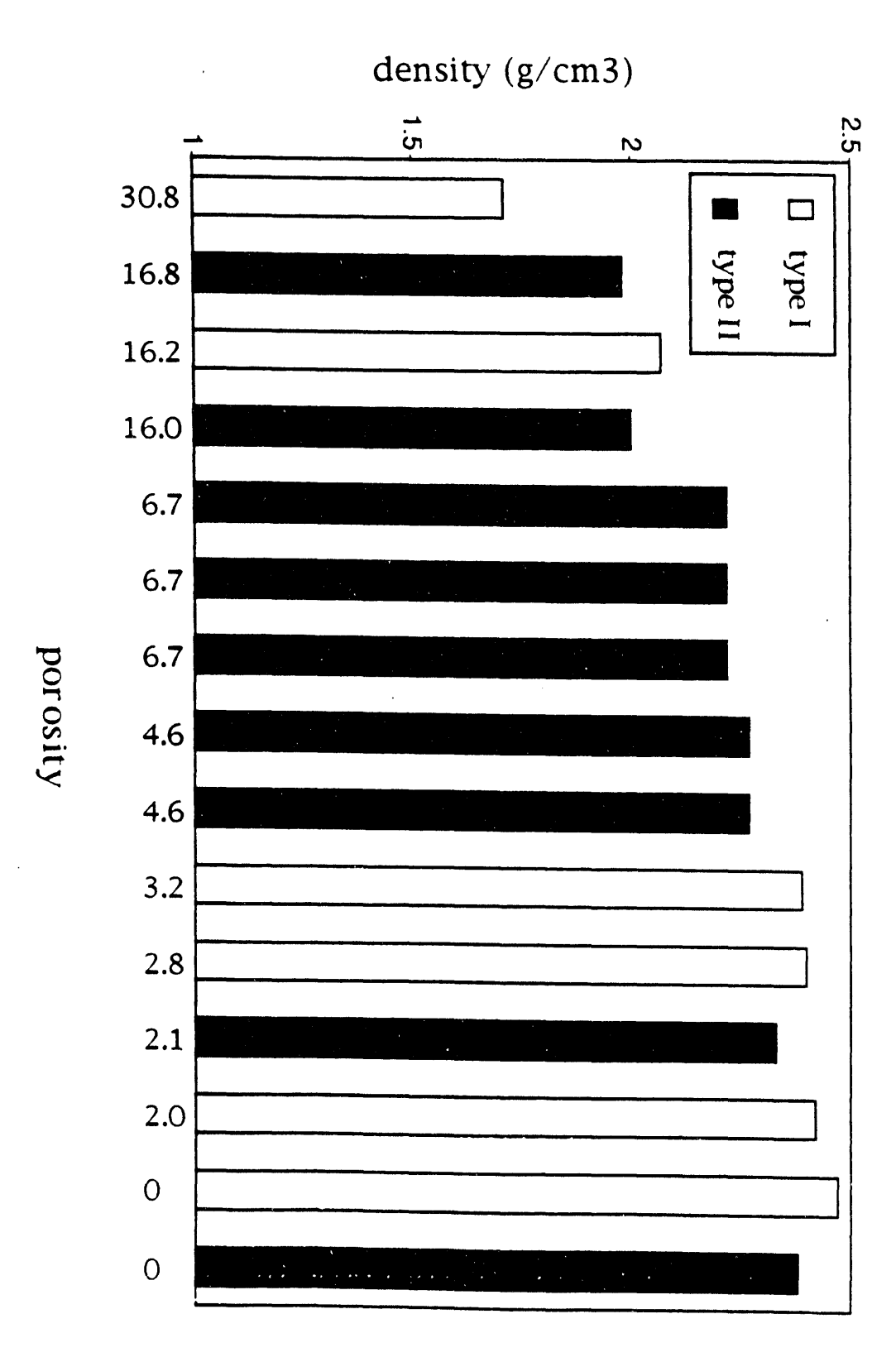
# Novarupta dome

The dome consists of rhyolite lava contaminated with mafic bands (Hildreth, 1987). Much of the dome lava has millimeter-scale layers of partially devitrified glass with small spherulites. The core of the dome is massively devitrified. The intermediate bands have dark brown glass and a greater percentage of groundmass crystals than other 1912 materials. When compared in thin section, glass color of the dark bands is most similar to andesite pumices and andesite clasts in breccias. Plagioclase is the dominant microphenocryst, but pyroxenes and magnetite are common.

#### Chemical Analysis

Whole rock analyses of breccias are consistent with proportions of 1912 rhyolite, dacite and andesite mentioned in the above breccia discussion. Heterogeneity among clasts appears greater in Type 1 than Type 2 breccia (Fig. 5). The pyroclastic dike is clearly not pure rhyolite (compare to rhyolite pumice values in Fig. 5). Composition of dark lava bands appears slightly more mafic than that typical for 1912 dacite.

Electron microprobe analysis of glass, plagioclases and pyroxenes in breccias confirms both types are composed primarily of 1912 magmas. Our analyses of pumice glass and phenocrysts agree well with data published by various authors (Avery 1992, Hildreth 1983, Westrich 1991). Figure 6a shows the average compositions and standard deviations of breccia glasses. Andesite, dacite and rhyolite pumice ranges are represented by stippled background fields. The majority of data points lie within the major pumice compositional ranges, but two other glass compositions are present in the breccias. Near 73 wt. % SiO2 is a field of data that represents andesite clasts with more crystalline groundmass than normal. Similar compositions are reported by Westrich et al. (1991) for andesite pumice. Occupying less volume in the breccias, but still important, is a tight data cluster at 76 wt. % SiO2. This 76 wt. % SiO2 composition corresponds to the mottled dark and clear glass noted above. Avery (1992) also reported one pumice clast from a late flow of the main valley-filling ignimbrite with this glass composition. Glass of the dike found in Type 2 breccia falls within the 1912 rhyolite magma



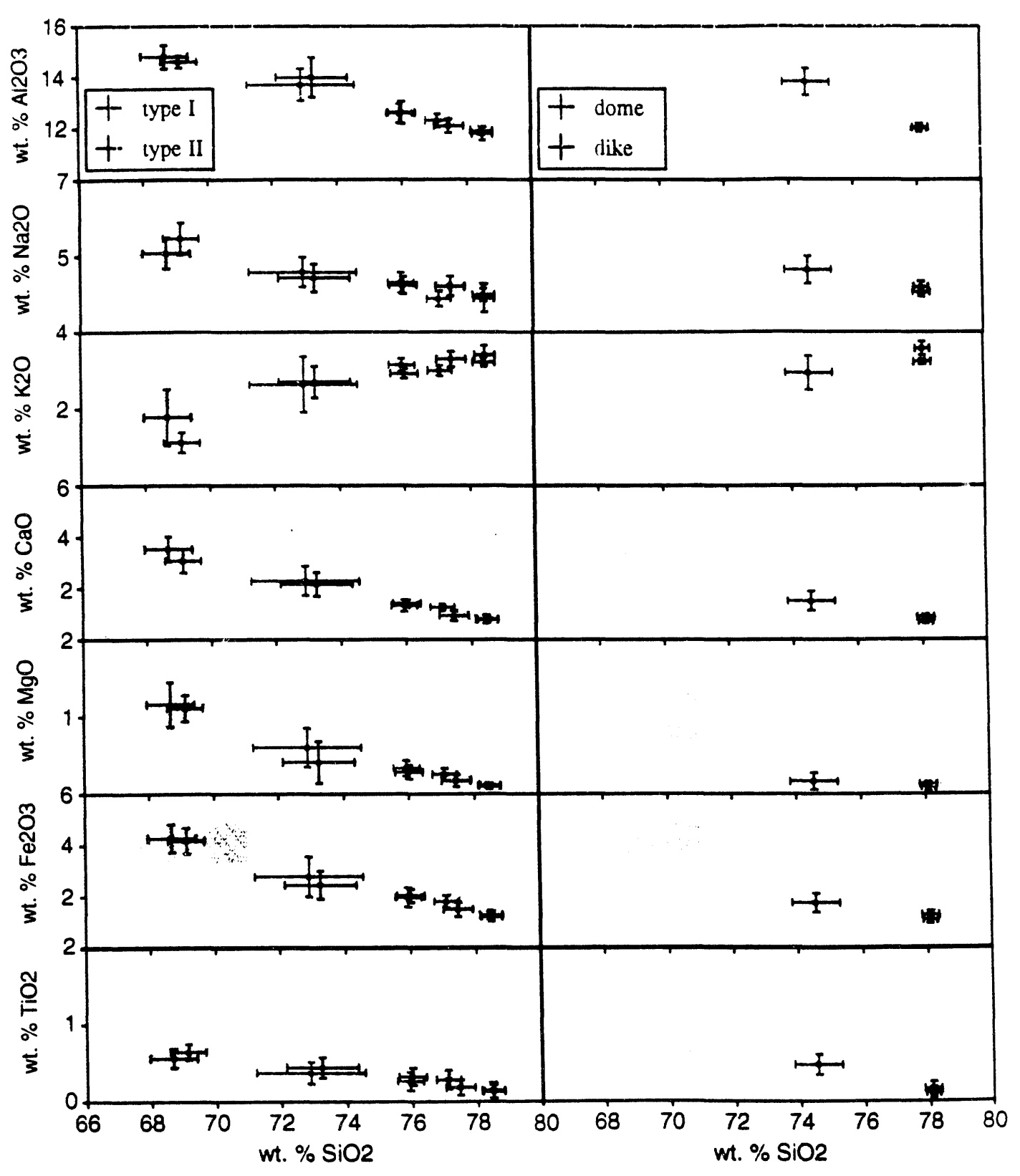
represents complete loss of pore space for that material. Figure 4. Density of breccia clasts is plotted against porosity. Porosity values assume densest sample of each type

Figure 5. Whole rock data was analyzed by XRF at Washington State University. Pumice values represent endmember compositions for the three Novarupta magmas. All other 1912 materials contain one or more of these magmatic components.

|                                |          |        | ;      | <b>1</b> | 1       |         |         | ,     | ı        |        |          | ļ        |       |
|--------------------------------|----------|--------|--------|----------|---------|---------|---------|-------|----------|--------|----------|----------|-------|
|                                | type I   | type I | type I | mixed    | type II | type II | type II | dike  | rhyolite | dacite | andesite | rhyolite | mafic |
|                                | ·JP··    | .,,,,  | 71     | type I   |         |         |         |       | pumice   | pumice | pumice   | lava     | lava  |
|                                |          |        |        |          |         |         |         |       |          |        |          |          |       |
| Normalized results (weight %): |          |        |        |          |         |         |         |       |          |        |          |          |       |
| SiO2                           | 66.82    | 63.62  | 68.64  | 64.28    | 64.30   | 63.55   | 64.46   | 72.54 | 77.55    | 65.85  | 61.68    | 77.49    | 64.53 |
| A12O3                          | 15.12    | 15.67  | 14.45  | 16.01    | 15.74   | 16.07   | 15.91   | 13.86 | 12.28    | 15.53  | 16.36    | 12.25    | 15.55 |
| TiO2                           | 0.48     | 0.59   | 0.43   | 0.65     | 0.65    | 0.70    | 0.61    | 0.34  | 0.15     | 0.66   | 0.71     | 0.15     | 0.61  |
| FeO*                           | 4.32     | 5.58   | 3.99   | 5.12     | 5.49    | 5.71    | 5.20    | 2.64  | 1.21     | 5.01   | 6.11     | 1.20     | 5.41  |
| MnO                            | 0.10     | 0.12   | 0.09   | 0.12     | 0.12    | 0.13    | 0.12    | 0.07  | 0.05     | 0.11   | 0.13     | 0.05     | 0.12  |
| CaO                            | 4.74     | 5.89   | 4.06   | 5.43     | 5.31    | 5.45    | 5.27    | 2.61  | 0.94     | 4.68   | 6.38     | 0.91     | 5.37  |
| MgO                            | 2.30     | 2.90   | 1.97   | 2.43     | 2.44    | 2.49    | 2.40    | 0.85  | 0.10     | 1.98   | 3.34     | 0.07     | 2.57  |
| K2O                            | 1.96     | 1.64   | 2.15   | 1.64     | 1.65    | 1.55    | 1.67    | 2.63  | 3.17     | 1.80   | 1.44     | 3.16     | 1.76  |
| Na2O                           | 4.08     | 3.89   | 4.15   | 4.22     | 4.18    | 4.25    | 4.25    | 4.42  | 4.54     | 4.26   | 3.74     | 4.71     | 3.98  |
| P2O5                           | 0.08     | 0.10   | 0.07   | 0.11     | 0.12    | 0.12    | 0.11    | 0.05  | 0.01     | 0.12   | 0.13     | 0.01     | 0.10  |
|                                |          |        |        |          |         |         |         |       |          |        |          |          |       |
| total                          | 99.78    | 98.47  | 99.34  | 98.45    | 99.58   | 97.63   | 99.24   | 98.92 | 97.86    | 99.41  | 99.52    | 99.17    | 99.13 |
|                                |          |        |        |          |         |         |         |       |          |        |          |          |       |
| Trace elements (ppm):          |          |        |        |          |         |         |         |       |          |        |          |          |       |
| <b>NI*</b>                     | 11       | 13     | 9      | 7        | 8       | 5       | 4       | 12    | 12       | 8      | 9        | 8        | 8     |
| Ni                             | 22       | 31     | 21     | 16       | 18      | 14      | 17      | 2     | 0        | 14     | 27       | 4        | 18    |
| Cr                             | 15       | 20     | 13     | 19       | 20      | 16      | 15      | 8     | 6        | 15     | 19       | 4        | 17    |
| Sc                             | 100      | 143    | 84     | 136      | 134     | 131     | 119     | 37    | 1        | 109    | 159      | 4        | 128   |
| V                              | 611      | 512    | 673    | 512      | 541     | 504     | 553     | 808   | 920      | 583    | 457      | 923      | 548   |
| Ba                             | 41       | 35     | 45     | 32       | 35      | 33      | 34      | 57    | 66       | 37     | 31       | 65       | 37    |
| Rb                             | 218      | 255    | 188    | 255      | 257     | 268     | 255     | 149   | 68       | 240    | 281      | 65       | 242   |
| Sr                             | 121      | 120    | 123    | 133      | 137     | 134     | 125     | 149   | 139      | 152    | 125      | 141      | 129   |
| Zr                             | 32       | 28     | 34     | 29       | 30      | 29      | 31      | 38    | 45       | 32     | 27       | 45       | 31    |
| Y<br>2                         | 58       | 63     | 53     | 77       | 65      | 73      | 69      | 45    | 36       | 66     | 68       | 34       | 65    |
| Zn<br>La                       | 36<br>16 | 8      | 29     | 2        | 3       | 16      | 10      | 5     | 19       | 9      | 21       | 19       | 10    |
| La<br>Co                       | 39       | 13     | 34     | 23       | 38      | 39      | 31      | 39    | 36       | 36     | 32       | 55       | 45    |
| Ce                             | 39<br>4  | 4      | 4      | 2        | 4       | 1       | 3       | 4     | 5        | 4      | 4        | 2        | 2     |
| Th                             | 4        | -+     | 7      | · - 1    | •       | -       | ٠,١     |       | ı        |        | 1        |          |       |

Figure 6. Glass analysis was conducted by electron microprobe at University of Alaska, Fairbanks. Andesite, dacite and rhyolite magmas have distinct glass compositions. Shaded background fields in each graph represent pumice glass ranges (within 2 $\sigma$  of the average) for the three magmas. Averages of data clusters are plotted for both types of breccia, pyroclastic dike material and dome lava (error bars are

20). Note the composition which fall outside typical pumice ranges. Dark glasses in type I breccia actually grade from 68 to 75 wt.% SiO2 and do not form two distinct data clusters.



field. Figure 6b also shows glass analyses of Novarupta Dome in relation to pumice glass compositions. The light gray glass falls neatly in the rhyolite pumice field, however the glass in the mafic material lies approximately equidistant between SiO2 contents of andesite and dacite glasses.

In Figure 7, stippled fields identify distinct anorthite composition ranges of plagioclase rims for each magma Type. Plagioclase phenocrysts in Type 1 and 2 breccias have anorthite rim contents appropriate for 1912 rhyolite, dacite and andesite. Plagioclases in the pyroclastic dike were derived from both rhyolite and andesite magmas. In dome rhyolite, plagioclase phenocrysts all fall in the rhyolite field. Plagioclase rims in mafic dome bands appear related to be andesite magma. Note that dome and dike materials are the only 1912 products to completely lack evidence of a dacitic component.

Pyroxene compositions in breccias are also typical of 1912 ejecta. Orthopyroxene composition ranges in pumices (Avery, 1992) distinguish rhyolite from other components and are compared to analyses of breccia pyroxenes in Figure 8. Phenocrysts of both breccia types fall in rhyolite and dacite/andesite ranges. Pyroclastic dike orthopyroxenes are in the dacite/andesite compositional field.

Type 1 breccia retains slightly more  $H_2O$  than Type 2, but both breccias are strongly degassed (Fig. 9a). Even rinds of bread crusted Type 2 bombs have <0.2 wt. %  $H_2O$ . The breccia block containing the pyroclastic dike has about twice the  $H_2O$  measured in other Type 2 clasts, although it does not increase with proximity to the dike (Fig. 9b). The dike itself with 0.9 wt. %  $H_2O$  is the least degassed material in this sample suite. Novarupta dome lavas, at < 0.1 wt. %  $H_2O$ , are completely degassed to a value appropriate for surface conditions.

# Crystallinity of andesite

Mafic magmas commonly undergo crystallization in response to incorporation in a cooler silicic host (Eichelberger, 1978, 1980). We examined andesite samples showing different relationships to rhyolite or dacite - separate andesite pumice, thin andesite bands in silicic pumice, thick andesite bands in silicic pumice, andesite in vent breccia, andesite in lava - for evidence of this crystallization response. Work was begun to quantify crystallinity, through analysis of back-scattered electron images acquired on the electron microprobe. Figure 10 shows a significant increase in groundmass crystallinity in andesite in lava relative to that in tephra, which we interpret to reflect more prolonged contact of the two magmas at elevated temperature. This is in accord with the more siliceous glass composition of andesite in lava, also an effect of more advanced crystallization. The generally dacitic bulk composition of the andesite-derived inclusions evident in both Hildreth's (1983) data and in ours appears to reflect fine mechanical intermixing with rhyolite, evident in thin section.

#### Summary and discussion

# General characteristics and occurrence

Breccia fragments in the 1912 deposits of Novarupta group into two distinct types. Type 1 breccia contains a heterogeneous assemblage with rhyolite and andesite more common than dacite. A fairly homogeneous aggregate of dacite with minor andesite and rhyolite comprises Type 2 breccia. Type 2 pumice clast sizes consistently average larger than those of Type 1 breccia, which includes traces of micron-scale glass shards. Type 1 is strongly welded except for fragments in late ash flows; Type 2 clasts range from weak agglomerates of pumice and lithics to densely welded blocks. Type 2 forms a significant component in deposits of the eruption's second and third days while Type 2 merely litters the surface.

Figure 7. Plagioclase analyses were conducted by electron microprobe at University of Alaska, Fairbanks. Andesite, dacite and rhyolite magmatic components can be identified by distinct ranges of plagioclase rim compositions. Shaded background fields represent ranges of plagioclase rim compositions established by Avery's (1992) extensive pumice analyses. Each point represents the rim of a single phenocryst with a line extending to the core composition.

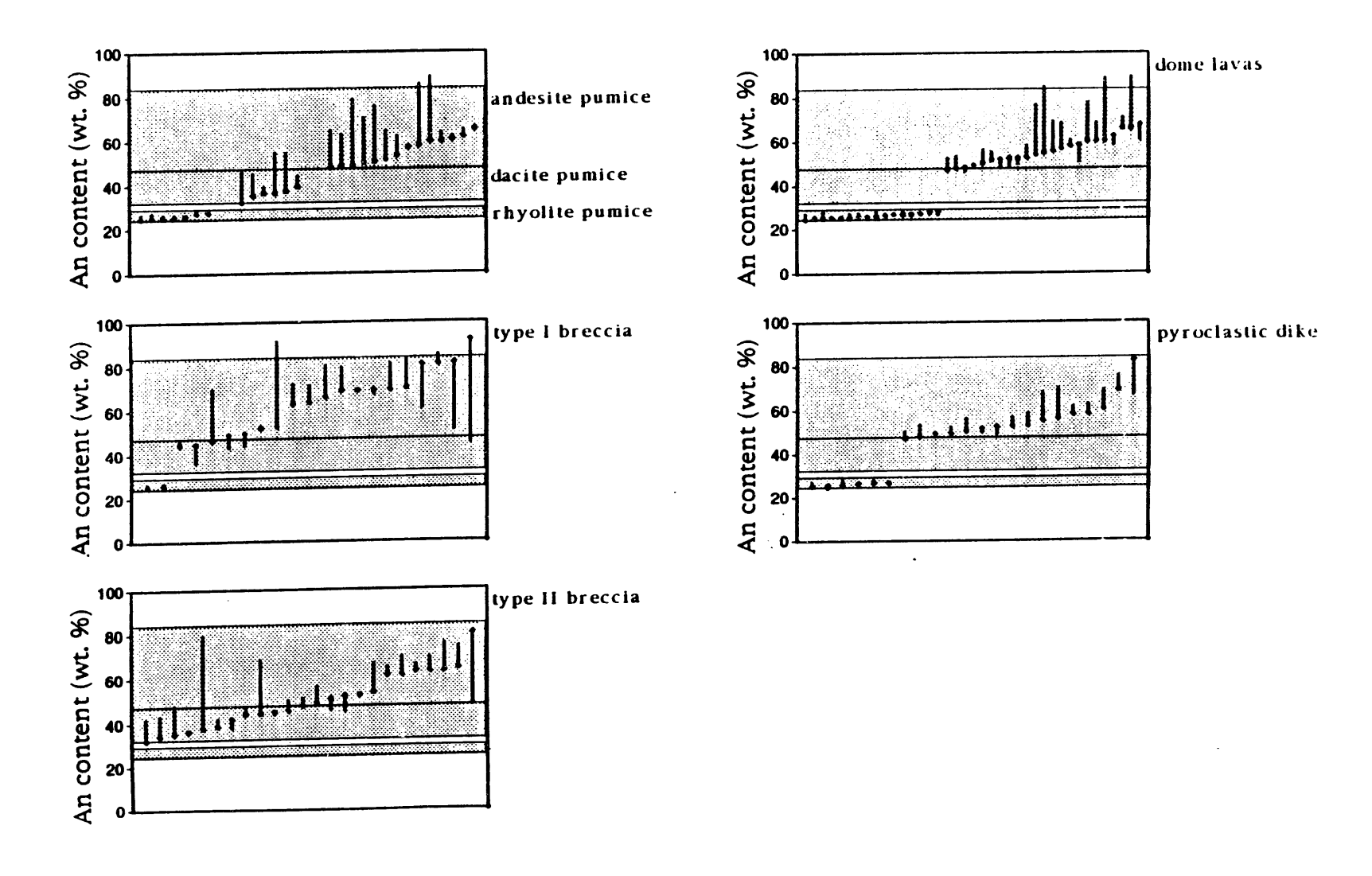
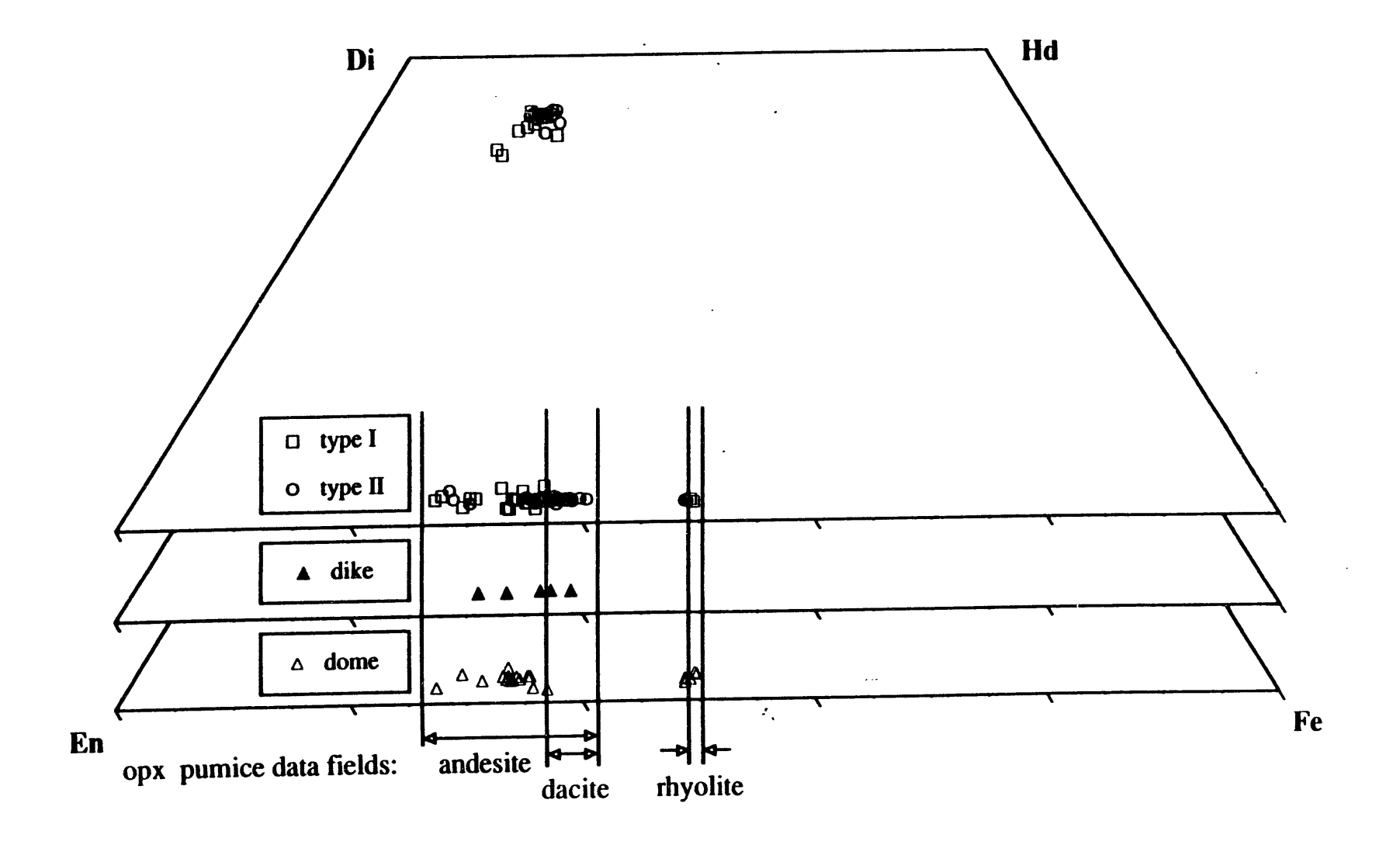
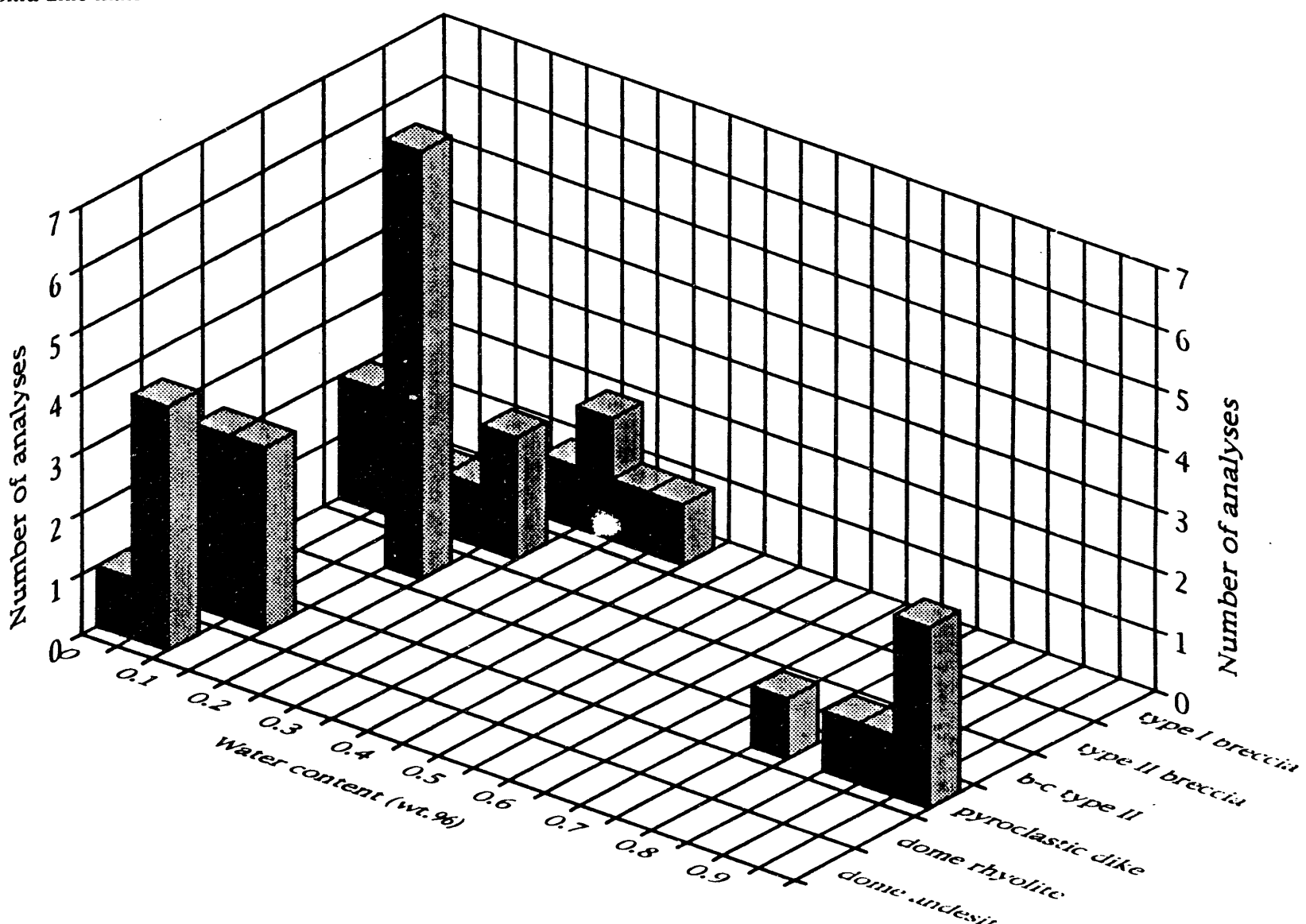


Figure 8. Pyroxene analyses were conducted by electron microprobe at University of Alaska, Fairbanks. Enstatite-ferrosilite ratios of orthopyroxene rims also indicate the presence of individual magmatic components. Heavy lines bound each magma type's range of compositions. Note the dacitic range lies within the andesitic field.



GI 91-91t

Figure 9. Water contents were determined by Karl Fischer titration using the total water method described by Westrich (1987). The Karl Fischer titrator at University of Alaska, Fairbanks was tested for accuracy using samples provided by Westrich; data agreed with Westrich's original results. a.) comparison of breccia types I and II, the rind of a large bread crusted (b-c) bomb of type II breccia, dome lavas and tephra dike material.



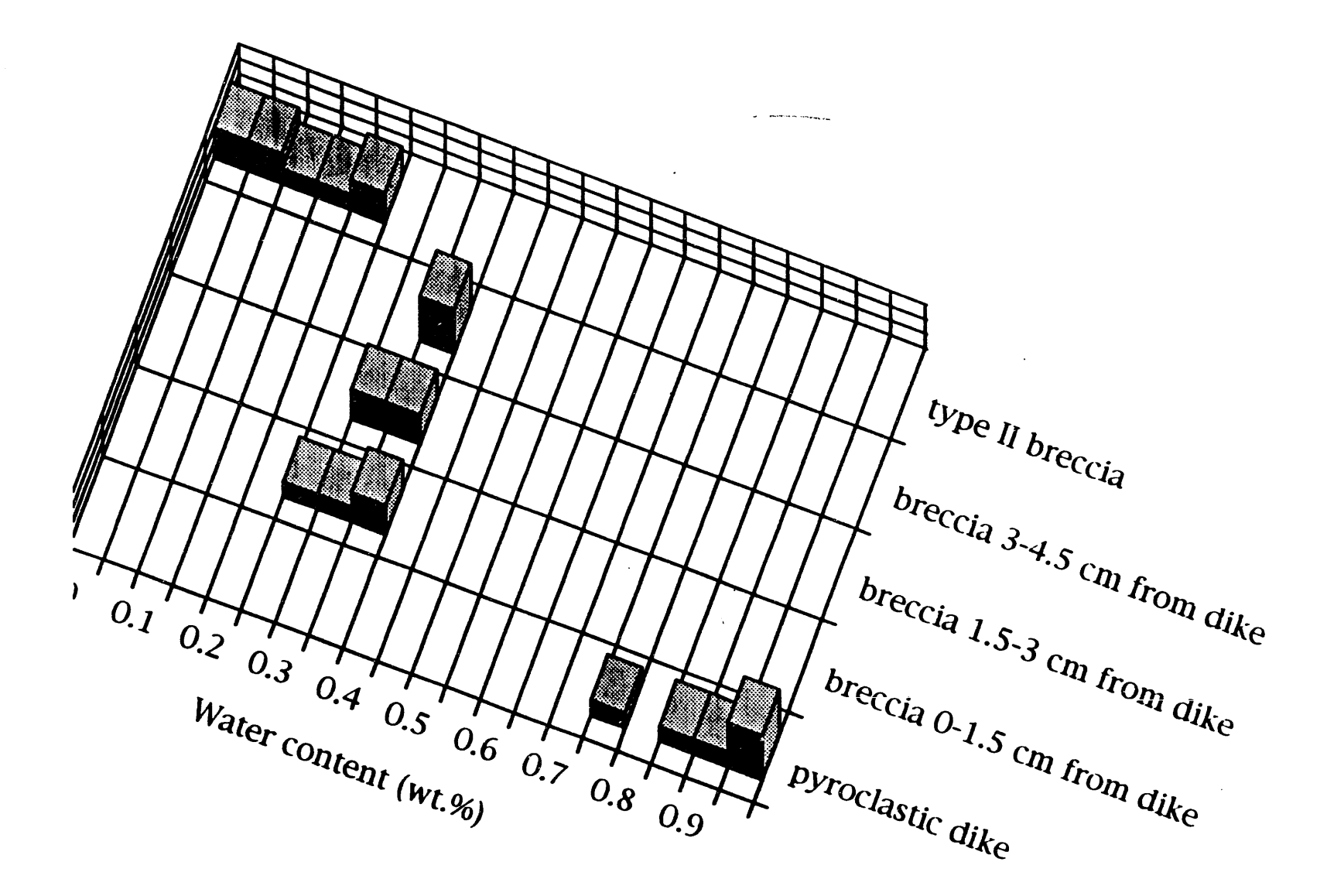
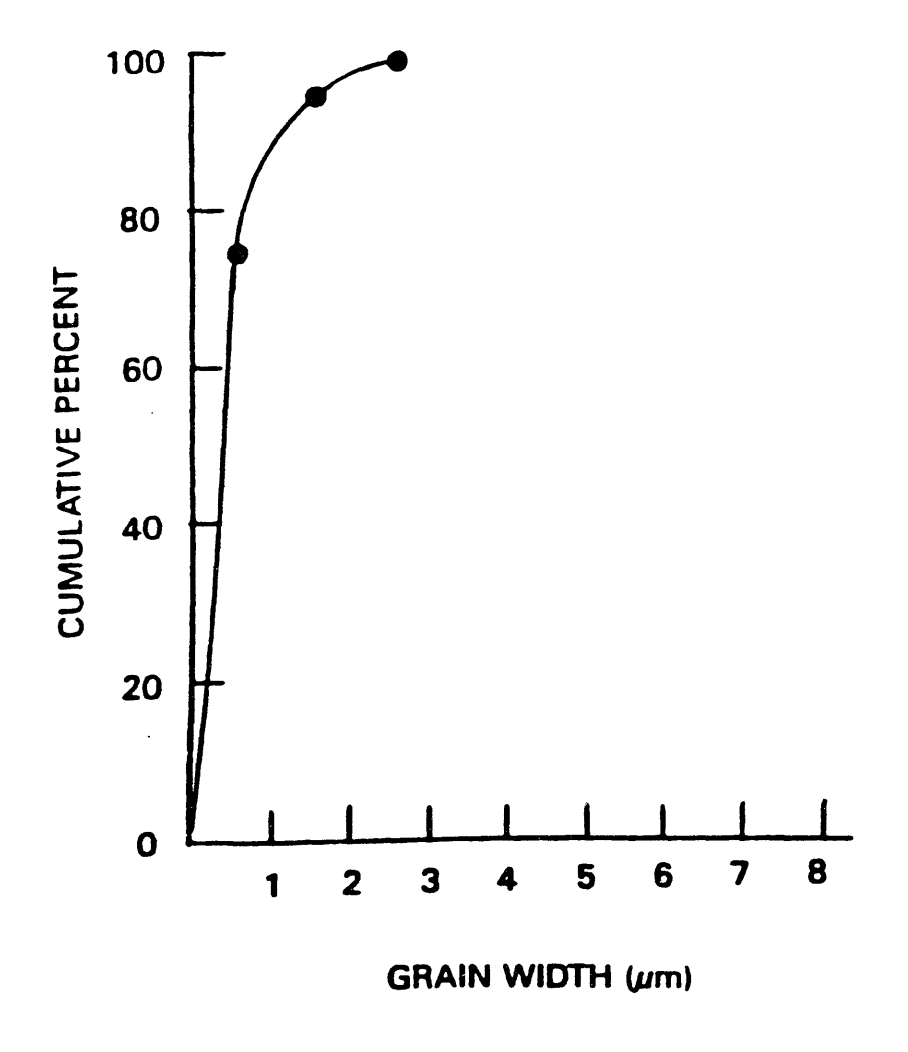
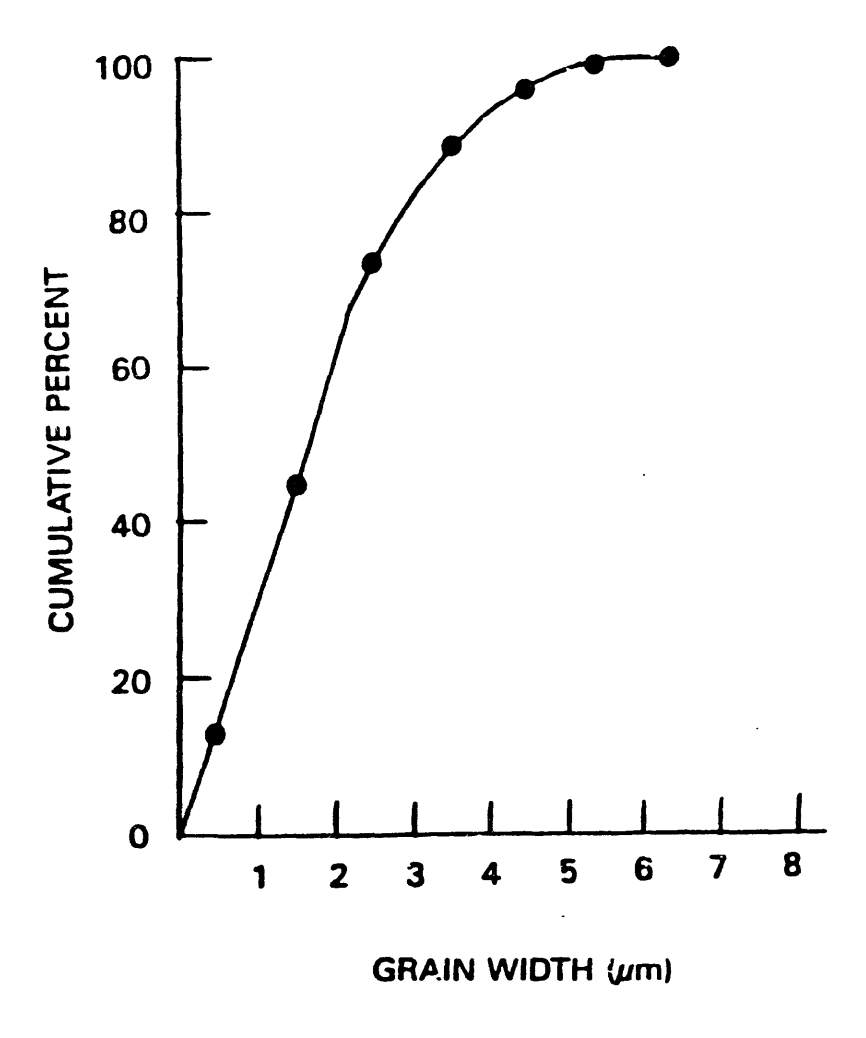


Figure 10. Grain size distribution of a) 1 cm andesite band in banded pumice from ashflow and b) dense andesite from Novarapta dome.







# Composition and source

Volcanic components in the breccias were compared to pumice in 1912 air fall and ash flow deposits. It is clear that the breccias are composed dominantly of 1912 material. This is true even of Type 1, where abundant andesitic clasts might be expected to include older Trident lavas. The fact that true lithics (non-1912 material) are restricted to Falling Mountain, which collapsed into the vent early in the eruption, and to Naknek Formation confirms what can be suggested from the surface: that the vent was primarily excavated in Naknek basement. The main heterogeneous valley-filling ignimbrite (VFI) contains rhyolite > dacite > andesite with late interspersed andesite > rhyolite > dacite flows (Fierstein and Hildreth, 1992). Type 1 most closely matches this late material, suggesting that it represents constriction of the vent late in Episode I. The earliest all-rhyolite deposits could not be the source for Type 1 breccia. Barely welded fragments of Type 1 first appear late in Episode I in the main VFI and dense clasts are found at the base of Episode II deposits. That Type 1 is the dominant "lithic" component of Episodes II and III supports the contention that the Episode II and II vent was excavated within the Episode I vent, in material represented by the Type 1 breccia.

Deposits of Episodes II and III are dominantly dacitic with minor andesite and rhyolite occurring in intraplinian pyroclastic flows (Fierstein and Hildreth, 1992). Dacite-rich Type 2 breccia correlates to these final deposits. However, because there was no chemical pattern of change during the eruption and because Type 2 breccia was only ejected at the end of the eruption, we can not assign the beginning of backfilling of the vent to a particular period of Episode II and III. A logical guess would be that like Type 1, it developed during the waning phase of activity.

# Comparison of Types 1 and 2

It is important to note some similarities and differences between Types 1 and 2. Both breccia types are enriched in andesite relative to the surface deposits with which they best correlate. This enrichment may be due to the sluggish nature of andesitic tephra and more explosive activity of rhyolite and dacite material as observed in the main deposits by Fierstein and Hildreth (1992). This does not necessarily imply a sorting process by magma type within the vent. Rather, eruptive phases with a higher proportion of andesitic material would have been less energetic, and because they were passing through a vent structure "too large" for them formed in earlier more energetic phases, would have tended to deposit material on the vent walls rather than to further erode the walls. Type 1 was ejected continuously during Episode II/III, whereas Type 2 was ejected in an apparently single, late, probably phreatic explosion. The tendency for Type 1 to be more welded and more water-rich may reflect a deeper sampling by vent-excavation rather than shallow phreatic disruption.

# Comparison of breccias with ignimbrites

Novarupta vent breccias are not ignimbrites. Similarities exist because some ignimbrites also fill vents and weld. However, vent breccias consist of a limited portion of tephra erupted and lack textures common to ash flow deposits. Ignimbrite pumice clasts typically have frayed edges on elongated ends (Ross and Smith, 1961). Pumice inclusions in vent breccias have rounded ends. Ash flow deposits usually possess significant proportions of fine particles. Ash and dust particles are notably scarce in both breccia types. Presumably fines are winnowed out by strong gas flow in the vent, or alternatively the breccias form at a depth where fragmentation is incomplete and the full complement of fines has not yet been generated. Breccias contain ~ twice the amount of lithics reported for the ignimbrite by Fierstein and Hildreth (1992). If the welded breccias formed from pooled pyroclastic flows, compositions correlating to all ignimbrite phases of the eruption would be expected. Continuous outflow of material through a small

funnel-shaped vent prevents ignimbrites from pooling in the crater. We conclude that at least the Type 1 breccia and probably some of Type 2 represents pyroclastic material aggraded or "plated out" at depth on vent walls rather than simple fall-back.

# Timing of welding of breccias

Densely welded Type 1 breccia is present in the earliest of Episode II deposits. We note that similar but incompletely welded material is present in late Episode I deposits. Following reasoning of Fierstein and Hildreth (1992) regarding timing of appearance of significant andesite in Episode I and the delay between eruption at Novarupta and fall at Kodiak, time required for welding of Type 1 material is constrained to  $\leq 5$  h. We note, however, that the early Type 1 breccia may be revesiculated (vesicles are round) rather than incompletely welded (in which case vesicles should show flattening). Welding may therefore have been instantaneous, as the material was plastered on the vent wall. This is perhaps more in accord with differences in flattening of magmatic clasts in Type 1 breccia. Less complete welding of some Type 2 material may likewise reflect sampling of incompletely welded material due to a short time between formation in Episode II/III and ejection in a late explosion - a local event for which there is no hard time constraint. Alternatively, most of the welding may have been instantaneous, but the late, shallow explosion may have simply sampled some very shallow non-welded vent fill.

# Timing of quenching of breccias

Vent breccia with as little as 0.15 wt. % H<sub>2</sub>O is bread crusted, demonstrating vesiculation after fragmentation and ejection. We infer therefore that breccias with the same or larger amounts (up to 0.40 wt. % observed for both Type 1 and 2) of retained water must have been pre-cooled to prevent vesiculation upon decompression. The relatively low content of lithics in Type 1 and negligible content in Type 2 implies that these breccias formed at magmatic temperatures and ejection at magmatic temperature would surely result in vesiculation (e.g., Westrich and Eichelberger, 1993). Hildreth (1983) calculates titanomagnetite-ilmenite equilibrium temperatures for rhyolite (805-850°C), dacite (855-955°C), andesite (955-990°C). Assuming mean temperatures for each magma and a lithic temperature of 0°C and using magma proportions given above, temperature of Type 1 is 920°C and temperature of Type 2 is 930°C. For Type 1 and applying reasoning from Fierstein and Hildreth's time constraints mentioned above, cooling must have occurred within about 5 hours of formation. Only rapid invasion of cold groundwater into the Episode I vent could have accomplished significant cooling on such a time-frame. For Type 2 breccias, no such time constraint on cooling can be placed, because Type 2 fragments wholly overlie the 1912 tephra deposits. However, we note that broadly similar composition glass in Novarupta began to devitrify before emplacement of the dome was complete, as indicated by the exposure of devitrified lava in rifts with openings of tens of meters. Emplacement of the small dome likely required days to at most weeks. Hence, devitrification began within weeks and undevitrified vent breccia must have been cooled at depth within weeks of formation. Certainly, if groundwater invaded the Episode I vent within hours of its formation, a similar event would probable have occurred after the close of Episode III. Ejection could have occurred later, but the simplest hypothesis is that this cooling event also produced the phreatic explosions that brought Type 2 vent-filling breccia to the surface.

#### Pyroclastic dike

This unique material provides the only evidence we have of the timing of emplacement of Novarupta Dome and poses an interesting possibility for shallow dike emplacement. Because the dike crosscuts and esite-rich Type 2 material (and therefore could not be Episode I material) and petrologically matches Novarupta Dome, it likely is related to emplacement of Novarupta Dome. Retained water contents are appropriate for formation at a few hundred meters depth, assuming water vapor pressure equal to lithostatic load. Such an assumption is reasonable, as

hydrofracturing required for emplacement of the dike as a dusty gas requires vapor pressure exceeding lithostatic load (shallower emplacement is therefore possible; deeper emplacement is possible if the vapor were not pure  $H_2O$ ). We infer that this dike is an offshoot of the conduit that fed Novarupta, or perhaps an early tip of the rising and degassing Novarupta intrusion. Applying the reasoning of the previous section, this would imply that emplacement of Novarupta Dome immediately followed cessation of the Episode III tephra eruption. The only other constraint on Novarupta's age is that Griggs saw it in 1916.

Were it not for the special circumstance of rapid in situ quenching, the pyroclastic nature of this dike would probably not be evident, that is the shard and fiamme texture would have been annealed out. This should be especially true give the elevated water content and hence relatively low viscosity of the glass. Had such a process occurred, the dike would have appeared as a normal rhyolitic dike, with no evidence of its fragmental origin. We must therefore ask whether many thin silicic dikes may not be welded products of hydrofracturing by dusty magmatic gas. Such a mechanism would remove the need to appeal to huge driving forces for injection of highly viscous magma into small dikes (Carrigan et al., 1992).

# Magma mixing

The mafic bands in Novarupta dome are andesitic. Whole rock data creates confusion because the mafic composition appears closest to dacite values. However when mafic material is viewed under the microscope even the purest mafic band is visibly intermixed with rhyolite lava on the finest scale. Analysis of the glass by electron microprobe places the mafic dome material more end between andesite and dacite values. Plagioclase data fall almost exclusively within andesitic ges. Microphenocrysts are more abundant in mafic dome lava than andesite in pumice or acia. Cooling due to mixing with rhyolite magma induced significant groundmass crystallization of plagioclase in andesite. The glass of the andesite magma became more silicic in response to losing the plagioclase components. Andesite clasts in the vent breccias establish the beginnings of a trend toward crystallization in response to mixing and toward increasingly siliceous glass with increasing groundmass crystallinity. Thus the response began within hours of the mixing, but it is much more fully developed in the dome lava where at least days were available for interaction before quenching.

- Avery V (1992) A petrogenetic study of the dacite from the 1912 eruption of Novarupta, Katmai National park, Alaska: implications for magma storage locations. M.S. thesis, University of Alaska, Fairbanks
- Carrigan, CR, Schubert G, Eichelberger JC (1992) Thermal and dynamical regimes of single-and two-phase magmatic flow in dikes. J. Geophys. Res., 97: 377-392
- Curtis GH, (1968) The stratigraphy of the ejecta from the 1912 eruption of Mount Katmai and Novarupta, Alaska. In: R. R. Coats, R. L. Hay, and C. A. Anderson (Editors), Studies in Volcanology. Geol. Soc. Am., Mem., 116: 153-210
- Eichelberger JC, Hildreth W, Papike J (1991) The Katmai Scientific Drilling Project, surface phase: investigation of an exceptional igneous system. Geophys Res Lett 8: 1513-1516
- Eichelberger JC (1978) Andesitic volcanism and crustal evolution. Nature 275: 21-27
- Eichelberger JC (1980) Vesiculation of mafic magma during replenishment of silicic magma resevoirs. *Nature* 288: 446-450
- Fierstein J, Hildreth W (1992) The plinian eruptions of 1912 at Novarupta, Katmai National park, Alaska. Bull Volcanol 54: 646-684
- Goodliffe A, Stone D, Kienle J, Kasameyer P (1991) The vent of the 1912 Katmai eruption: gravity and magnetic measurements. Geophys Res Lett 8: 1521-1524
- Griggs RF (1922) The Valley of Ten Thousand Smokes. National Geogr Soc, Washington, 340 pp
- Hildreth W (1983) The compositionally zoned eruption of 1912 in the Valley of Ten Thousand Smokes, Katmai National Park, Alaska. J Volcanol Geotherm Res 18: 1-56
- Hildreth W (1987) new perspectives of the eruption of 1912 in the Valley of Ten Thousand Smokes, Katmai National Park, Alaska. Bull Volcanol 49: 680-693
- Ross C, Smith R (1961) Ash-flow tuffs: their origin geologic relations and identification. USGS Prof. Paper 366, 81 pp
- Westrich H (1987) Determination of water in volcanic glasses by Karl-Fischer titration. Chem Geol 63: 335-340
- Westrich H (1991) Degassing of the 1912 Katmai magmas. Geophys Res Lett 8: 1561-1564
- Westrich H and Eichelberger JC (1993) Gas transport and bubble collapse in rhyolitic magma: an experimental approach. in preparation

# 

· . ,